analytical chemistry

Article

pubs.acs.org/ac

Manganese Porphyrin-dsDNA Complex: A Mimicking Enzyme for Highly Efficient Bioanalysis

Jie Xu,[†] Jie Wu,*[,†] Chen Zong,[†] Huangxian Ju,*[,†] and Feng Yan[‡]

[†]State Key Laboratory of Analytical Chemistry for Life Science, Department of Chemistry, Nanjing University, Nanjing 210093

[‡]Jiangsu Institute of Cancer Prevention and Cure, Nanjing 210009, P.R. China

Supporting Information

ABSTRACT: Manganese porphyrin (MnTMPyP)−dsDNA complex was reported as an excellent mimicking enzyme of peroxidase. It possessed high catalytic activity and much quicker catalytic kinetics and better stability with exposure to light irradiation and high temperature than both horseradish peroxidase and hemin/G-quadruplex DNAzyme. The groove binding of MnTMPyP to the dsDNA scaffold efficiently maintained the catalytic activity of the MnTMPyP center and improved its stability. By combining with an isothermal hybridization chain reaction (HCR) and in situ formation of MnTMPyP-dsDNA, a highly efficient chemiluminescent (CL) immunosensing method was proposed. After a sandwich immunoreaction, a biotinylated DNA strand, which was bound to biotinylated signal antibody by streptavidin, triggered the HCR and growth of MnTMPyP-dsDNA on the immunocomplex. The in situ, HCR-assisted enzyme formation brought numerous enzymatic catalytic centers, MnTMPyP, on the immunocomplex, resulting in significant CL signal amplification and highly sensitive CL detection. Using carcinoembryonic antigen as the model target, the proposed CL immunoassay method showed a wide linear range from 10 pg/mL to 100 ng/mL with a detection limit of 6.8 pg/mL. The new MnTMPyP-dsDNA complex could be conveniently synthesized, functionalized, and combined with DNA amplification strategies, showing a promising potential in bioanalysis and other relative fields.

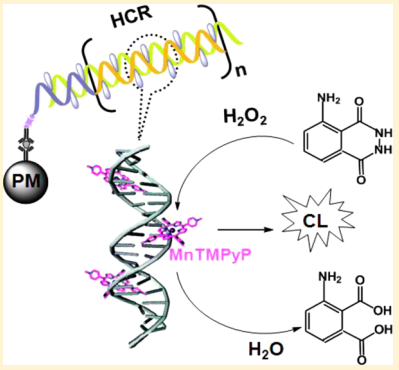

Artificial mimicking enzymes that possess high catalytic activity and distinct substrate selectivity are highly desired for developing new catalytic reactions and bioanalysis systems due to their simpler syntheses and preparation, better stability, and easier modification than natural enzymes.[1−3] As the catalytic centers of many enzymes, porphyrins, especially metalloporphyrins, have been widely used for the development of artificial enzymes.[4−6] For example, hemin, an iron protoporphyrin, has become one of the most used metalloporphyrins for the preparation of horseradish peroxidase (HRP) mimics.[7] Because hemin can undergo molecular aggregation to form catalytic inactive dimers in aqueous solution,[8] a variety of materials such as hydrogel,[9,10] protein,[11,12] graphene,[3,13,14] and DNA[15] have been used to provide it with a protein-like microenvironment for improving its stability and activity in the construction of mimicking enzymes. Specifically, an interesting DNAzyme with peroxidase-like activity can be formed by the conjugation of a single-stranded guanine-rich nucleic acid with hemin and used as a label in electrochemical,[16−18] calorimetric,[19] and chemiluminescent (CL)[20,21] bioanalysis. However, the DNAzyme can be quickly inactivated when it exposes to light irradiation. New mimicking enzymes which do not need special DNA sequence and dark condition during their usage are in urgent demand.

Manganese porphyrin, manganese(III) meso-tetrakis(4-*N*-methylpyridyl)-porphyrin (MnTMPyP) (Figure S1, Supporting Information), that contains manganese as the central metal atom has showed peroxidase-like activity[22] and much better catalytic performance than iron porphyrin.[23] Unfortunately, the labeling process of this mimicking enzyme to protein leads to a loss of its catalytic activity up to 50%, and the limited binding amount of MnTMPyP to each protein also limits its catalytic performance.[23] It has been reported that MnTMPyP can interact with both AT and GC base pairs of double-strand DNA (dsDNA) by groove binding,[24−27] while no interaction is observed between porphyrin and single-strand DNA (ssDNA). Such phenomena imply that dsDNA can be an excellent scaffold to capture MnTMPyP molecules without the need of specific sequence. Thus this work designed a new avenue for preparation of mimicking enzyme with peroxidase-like activity by loading MnTMPyP in the dsDNA scaffold. Moreover, the amount of MnTMPyP as the catalytic center in the scaffold was adjustable by changing the length of dsDNA.

Molecular biological amplification strategies such as polymerase chain reaction, rolling circle amplification, and hybridization chain reaction (HCR) have provided simple and effective biotechnologies for in situ adjustment of the length of dsDNA. For example, isothermal HCR, which was first introduced by Dirk and Pierce,[28] can carry out the polymerization of oligonucleotides into a long dsDNA spontaneously under

Received: January 9, 2013
Accepted: February 22, 2013
Published: February 22, 2013

   dx.doi.org/10.1021/ac4000688 | *Anal. Chem.* 2013, 85, 3374−3379

mild conditions in the presence of an initiator DNA. Here, by combining the interaction between MnTMPyP and dsDNA with HCR, a simple strategy for efficient signal amplification of the new artificial mimicking enzyme was proposed. As shown in Scheme 1, by labeling the initiator DNA to the product of

Scheme 1. Schematic Illustration of Amplifying Synthesis of MnTMPyP-dsDNA Enzyme Mimic as Label for CL Biosensing

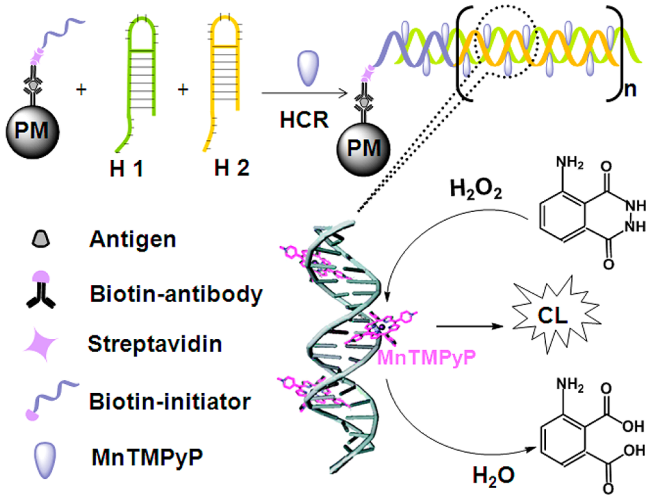

biorecognition reaction, such as immunoconjugate, the HCR process could be generated in situ on the immunocomplex, along with the growth of MnTMPyP-dsDNA mimicking enzyme. The immunoreaction and following HCR process could be performed on different supports. The numerous enzymatic catalytic centers, MnTMPyP, which were trapped on the immunocomplex with the HCR-assisted dsDNA production, could be combined with different detection techniques including chemiluminescent detection to carry out significant signal amplification and highly sensitive detection. The new MnTMPyP-dsDNA complex could be conveniently synthesized, functionalized, and amplified with DNA amplification strategies, showing great applicability in bioanalysis.

EXPERIMENTAL SECTION

Materials and Reagents. MnTMPyP was a gift from Kanazawa University (Japan). Capture antibody (mouse monoclonal antibody, clone no. bsm-1023) and biotinylated signal antibody (rabbit polyclonal antibody, clone no. bs-0719R-bio) of carcinoembryonic antigen (CEA) were purchased from Beijing Biosynthesis Biotechnology Co. Ltd. (China). A commercial CL ELISA kit for CEA, including the standard solutions with concentrations from 5 to 160 ng/mL and CL substrate solutions for HRP (luminol-*p*-iodophenol and H_2O_2), was obtained from Autobio Diagnostics Co., Ltd. (China). The corresponding electrochemiluminescent (ECL) immunoassay reagent kit for reference detection was provided by Roche Diagnostics GmbH (Germany). The aqueous suspension of paramagnetic silicon dioxide microspheres (PMs) coated with epoxy group (10 g/L, diameter 1−2 μm) was obtained from the Tianjin BaseLine Chromtech Research Centre (China). All the oligonucleotides, including the DNA initiator, H1 and H2 hairpins for HCR, S1 and S2 sequences for probing the interaction between MnTMPyP and dsDNA, and G-quadruplex for forming DNAzyme as control, were purchased from Sangon Biological Engineering Technology & Co. Ltd. (Shanghai, China), and their sequences are listed in Table S1, Supporting Information. The stock solutions of 10 μM initiator and two hairpins were prepared with Tris−HCl buffer (20 mM, pH 7.6). The coupling buffer for antibody immobilization was 0.01 M phosphate buffer solution (PBS, pH 7.4). PBS (0.01 M pH 7.4) containing 10 mM ethanolamine was used as the blocking buffer. Washing buffer was 0.01 M PBS spiked with 0.05% Tween-20 (pH 7.4). Tris−HCl buffer (20 mM, pH 7.6) containing 300 mM NaCl and 50 mM $MgCl_2$ was used for HCR. Ultrapure water obtained from a Millipore water purification system (≥18 MΩ, Milli-Q, Millipore) was used in all assays. Clinical serum samples were from Jiangsu Cancer Hospital. All other reagents were of analytical grade and used as received.

Apparatus. The circular dichroism (CD) spectra were obtained with a J-810/163-900 circular dichroism chiroptical spectrometer (Jasco, Japan). The ultraviolet−visible (UV−vis) spectroscopic experiments were performed with a UV-3600 UV−vis spectrophotometer (Shimadzu, Japan). The CL signals were recorded on an IFFM-E Luminescent Analyzer (Remax, China). The reference immunoassay was performed with a Roche Elecsys 2010 immunoassay analyzer (Roche Diagnostics GmbH).

Preparation of Anti-CEA Antibody Modified PMs. The immobilization process of anti-CEA antibody on PMs was performed according to the previous work.[29] A volume of 200 μL of PM suspension was washed with washing buffer three times using a permanent magnet to isolate them from the supernatant waste. The PMs were then resuspended in 1 mL of coupling buffer and mixed with 100 μL of anti-CEA antibody (1.0 mg/mL) for covalent linking under gentle stirring at room temperature for 2 h and then at 4 °C overnight. The resulting antibody immobilized PMs were thoroughly washed with washing buffer and then blocked with blocking buffer for 2 h. Finally, the antibody modified PMs were dispersed in PBS to a volume of 1.0 mL and kept at 4 °C before use.

Analytical Protocol. The whole assay was controlled automatically by a personal computer equipped with the IFFM software package. First, an equal volume of biotinylated CEA signal antibody (1 mg/mL) and streptavidin (1 mg/mL) solutions were mixed at room temperature for 30 min, followed by a 10-times dilution with pH 7.4 PBS buffer. A volume of 20 μL of the above solution was mixed with 20 μL of CEA sample and anti-CEA antibody modified PMs isolated from 40 μL of suspension and then introduced into the helical glass tube. After the mixture flowed back and forth at 37 °C for 10 min, the PMs were online separated using a permanent magnet and washed with washing buffer. A volume of 40 μL of 1 μM biotinylated initiator DNA was then introduced into the glass tube to mix with the immunocomplex immobilized PMs and incubated for 10 min. Following a washing step, 40 μL of mixture solution containing 0.5 μM hairpin H1, 0.5 μM hairpin H2, and 3 μM MnTMPyP was introduced into the glass tube to trigger the HCR and in situ form the complex of MnTMPyP-dsDNA on the sandwich immunocomplex. This reaction was terminated after 1 h and followed by a washing step. Finally, 80 μL of CL substrate mixture was delivered into the tube for recording the CL signal.

RESULTS AND DISCUSSION

Interaction of MnTMPyP with dsDNA. The formation of MnTMPyP-dsDNA complex was verified by CD and UV−vis

dx.doi.org/10.1021/ac4000688 | Anal. Chem. 2013, 85, 3374−3379

absorption spectra (Figure 1). Free MnTMPyP did not show any detectable CD absorption, while dsDNA showed both the

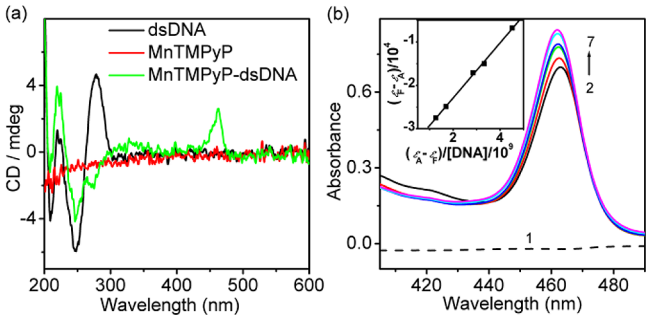

Figure 1. (a) CD spectra of 5.0 μM dsDNA, 100 μM MnTMPyP, and the mixture of 5.0 μM dsDNA and 90 μM MnTMPyP and (b) UV–vis spectra of 1.5 μM DNA (1) and the mixtures of 5.0 μM MnTMPyP and 0, 1.5, 4.5, 6.0, 14.6, and 21.6 μM DNA (2–7) in 10 mM pH 7.4 PBS. Inset: plot of $\varepsilon_F - \varepsilon_A$ vs $(\varepsilon_A - \varepsilon_F)/[DNA]$.

typical CD bands of the right-handed B-helix at 250 and 275 nm (Figure 1a).[30] After mixing MnTMPyP with dsDNA solution, the CD bands of dsDNA reduced, and a new positive induced CD absorption peak occurred at 462 nm, indicating the interaction between MnTMPyP and dsDNA to form the MnTMPyP-dsDNA complex.[24,25,27] The UV–vis spectrum of MnTMPyP showed a Soret absorption band at 463 nm. With the increasing concentration of dsDNA in MnTMPyP solution, the peak intensity increased and the peak slightly shifted to 462 nm, the same wavelength as the CD absorption peak of MnTMPyP-dsDNA (Figure 1b), further demonstrating the formation of the complex. The hyperchromicity and the positive induced CD band in the visible region indicated the groove binding of MnTMPyP to dsDNA. The binding constant, K, could be determined with the following eq 1:[24]

$$\varepsilon_F - \varepsilon_A = \frac{\varepsilon_A - \varepsilon_F}{[DNA]K} + \Delta\varepsilon \quad (1)$$

where ε_A is the absorbance of a given solution divided by the total MnTMPyP concentration, ε_F and ε_B are molar absorptivities of free and bound MnTMPyP, respectively, and $\Delta\varepsilon = \varepsilon_F - \varepsilon_B$. From the inset in Figure 1b, the K and ε_B values were obtained to be 1.58×10^5 M^{-1} and 1.75×10^5 M^{-1} cm^{-1}, respectively. The K value of MnTMPyP-dsDNA was similar to those of other porphyrin–dsDNA systems,[24,31−33] indicating the strong binding of MnTMPyP to dsDNA.

Catalytic Activity Test. The peroxidase-like catalytic activity of MnTMPyP-dsDNA was evaluated using an oxidation reaction of pyrogallol by H_2O_2.[9,14] The catalytic reaction was carried out with 5 μM MnTMPyP-dsDNA or hemin/G-quadruplex DNAzyme at 0.1, 0.2, 0.5, 1.0, and 2.0 mM pyrogallol and 40 mM H_2O_2. The reaction progress was monitored using UV–vis spectroscopy at 420 nm in the kinetic mode to measure the reaction rate V. The reaction process followed a conventional enzymatic dynamic regulation of the Michiaelis–Menten equation. The Michaelis constant K_M and catalytic constant k_{cat} were calculated by the Lineweaver–Burk plot (eq 2) as shown in Figure 2:

$$\frac{1}{V} = \frac{K_M}{V_{max}}\frac{1}{[S]} + \frac{1}{V_{max}} \quad (2)$$

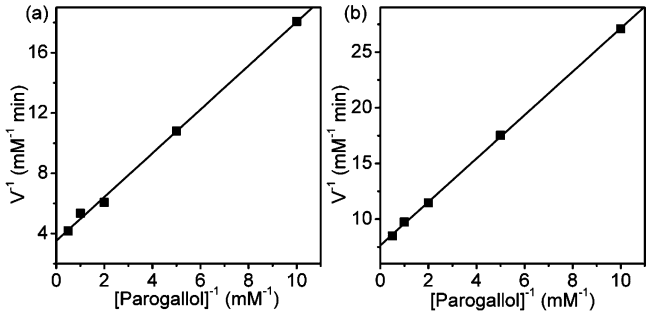

Figure 2. Lineweaver–Burk plots of pyrogallol oxidation catalyzed by (a) 5 μM MnTMPyP-dsDNA and (b) 5 μM hemin/G-quadruplex DNAzyme in the presence of 40 mM H_2O_2.

From the Lineweaver–Burk plot, the Michaelis constant K_M and the catalytic constant k_{cat} of MnTMPyP-dsDNA in pyrogallol oxidation reaction were calculated to be 0.41 mM and 56.8 min^{-1}, respectively. The k_{cat} value doubled that of hemin/G-quadruplex DNAzyme (Table 1), indicating the

Table 1. Kinetic Parameters for Pyrogallol Oxidation Reaction Catalyzed by Different Catalysts

catalyst	k_{cat} [min^{-1}]	K_M [mM]	k_{cat}/K_M [M^{-1} min^{-1}]	ref
MnTMPyP-dsDNA	56.8	0.41	1.4×10^5	this work
hemin/G-quadruplex DNAzyme	26.1	0.25	1.0×10^5	this work
hemin-graphene	246	1.22	2.0×10^5	14
FeTMPyP-antibody	680	8.6	7.9×10^4	11
HRP	1750	0.81	2.2×10^6	11

higher catalytic activity. The adjacent K_M values between MnTMPyP-dsDNA and DNAzyme implied their similar affinity. Although the k_{cat} value of the proposed MnTMPyP-dsDNA was smaller than those of HRP and its mimicking enzymes including hemin-graphene[14] and FeTMPyP labeled to antibody,[11] it showed better affinity and its catalytic efficiency (k_{cat}/K_M) was also higher than FeTMPyP labeled to antibody and similar to hemin-graphene.

Catalytic Kinetics of MnTMPyP-dsDNA Complex. The catalytic kinetics of MnTMPyP-dsDNA was investigated using the luminol-H_2O_2 CL reaction in a static mode. Upon addition of MnTMPyP-dsDNA to the mixture of luminol and H_2O_2, the CL reaction was immediately observed and the CL emission intensity increased quickly and reached its maximum value within 6 s (Figure 3). The CL reaction kinetics was obviously faster than those systems containing HRP or hemin/G-quadruplex DNAzyme, which reached the maximum value at around 70 and 25 s, respectively. The fast kinetics of MnTMPyP-dsDNA indicated that the proposed mimicking enzyme was suitable for dynamic detection and could be used as an excellent candidate of enzyme label in flow injection CL analysis and biosensing application. In the presence of 0.05 μM Mn(III)TMPyP-dsDNA or Fe(III)TMPyP-dsDNA, the luminol-H_2O_2 system showed a CL emission intensity of 39 or 36 kau, respectively, indicating slightly better catalytic ability of Mn(III)TMPyP-dsDNA than Fe(III)TMPyP-dsDNA.

Stability of MnTMPyP-dsDNA Complex. The main limitation of natural enzymes is their poor stability. Thus, a favorable mimicking enzyme should not only process the catalytic ability similar to natural enzymes but also maintain its

dx.doi.org/10.1021/ac4000688 | Anal. Chem. 2013, 85, 3374−3379

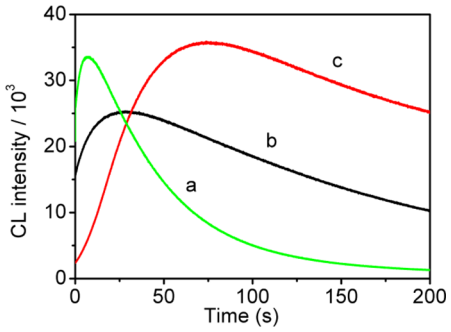

Figure 3. Kinetic behaviors of the luminol-H_2O_2 CL reaction catalyzed by (a) MnTMPyP-dsDNA, (b) DNAzyme, and (c) HRP.

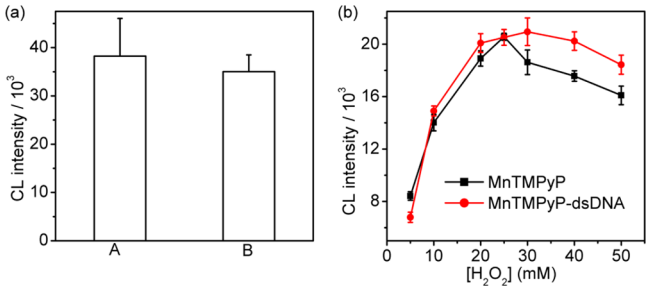

Figure 5. (a) CL intensities of the luminol-H_2O_2 system catalyzed by 0.05 μM of MnTMPyP (column A) and MnTMPyP-dsDNA (column B) and (b) effect of H_2O_2 concentration on CL intensity of the luminol-H_2O_2 system catalyzed by 0.01 μM of MnTMPyP and MnTMPyP-dsDNA.

activity in broad conditions. This work further investigated the effects of light irradiation, temperature, and alkaline conditions on the catalytic activity of MnTMPyP-dsDNA using a luminol-H_2O_2 CL reaction. Under light irradiation for 1 h, MnTMPyP-dsDNA maintained 89% of the initial catalytic activity, which was much higher than those of 19% and 20% for natural HRP and hemin/G-quadruplex DNAzyme, respectively (Figure 4a), indicating that the proposed MnTMPyP-dsDNA as an enzyme mimic possessed the unique feature of light insensitivity rather than HRP and hemin/G-quadruplex DNAzyme. Moreover, the MnTMPyP-dsDNA could keep its catalytic activity even at 60 °C, while HRP and hemin/G-quadruplex DNAzyme were more vulnerable to high temperature conditions, especially, HRP lost most (93%) of its catalytic activity at 60 °C (Figure 4b). At pH 9.0 1 h, HRP lost 58% of its catalytic activity, and both MnTMPyP-dsDNA and hemin/G-quadruplex DNAzyme displayed excellent stability (Figure 4c). Overall, the proposed MnTMPyP-dsDNA as enzyme mimic exhibited much better stability than both HRP and DNAzyme under light irradiation and high temperature and was more stable than HRP at high pH, showing potential applications in broad fields.

Now that the MnTMPyP-dsDNA complex was formed through groove binding of MnTMPyP to dsDNA scaffold without destruction of MnTMPyP, the complex should have the catalytic activity similar with the active center, MnTMPyP. The CL intensity of luminol-H_2O_2 reaction catalyzed by the complex showed 92% of the catalytic activity of MnTMPyP (Figure 5a). Moreover, at the H_2O_2 concentrations higher than 25 mM, the MnTMPyP-dsDNA system showed a further increase of CL intensity and then a slight decrease, but the MnTMPyP system showed a sharp decrease of CL intensity (Figure 5b), thus the dsDNA scaffold possessed better protective action and the binding of MnTMPyP to dsDNA scaffold led to a higher ability to resist the effect of H_2O_2, which generally occurs in the enzymatic reactions of HRP and its enzyme mimics.

Analytical Performance. As DNA can be conveniently modified with functional groups, such as biotin, carboxyl, and amino groups, the proposed mimicking enzyme can be easily labeled to biomolecules for construction of sensitive biosensing systems. To demonstrate its application in bioanalysis, here the MnTMPyP-dsDNA was formed using a biotinylated DNA strand, which was bound to biotinylated signal antibody by streptavidin, to produce a dsDNA scaffold. As shown in Scheme 1, the biotinylated signal antibody was bound on capture antibody modified PMs by the sandwich immunoreaction. The presence of PMs made it more convenient to separate immunocomplex for forming MnTMPyP-dsDNA and detecting CL emission. After the biotinylated DNA strand initiated an isothermal HCR process of H1 and H2 hairpins, a dsDNA strand containing plenty of MnTMPyP molecules could be formed on each immunocomplex, which led to a novel amplification strategy for highly efficient CL immunoassay.

Under optimal conditions of 1 h HCR time and 10-min incubation time (Figure S2, Supporting Information), the HCR amplification at 1.0 ng/mL CEA produced a CL emission of 2.1 times that in the absence of HCR, along with the similar noise (Figure S3, Supporting Information). Furthermore, the CL emission using MnTMPyP-dsDNA label coupled with HCR was 2.8 times that using the HRP label. The CL intensity of the proposed immunosensing system linearly increased with the increasing logarithm of CEA concentration in the range from 0.01 to 100 ng/mL with a correlation coefficient of 0.9993 (Figure 6). The limit of detection at 3 SD was 6.8 pg/mL, which was 1 order of magnitude lower than that without HCR amplification (Figure S4, Supporting Information), 1000 lower than that of MnTMPyP based CL immunoassay,[23] and

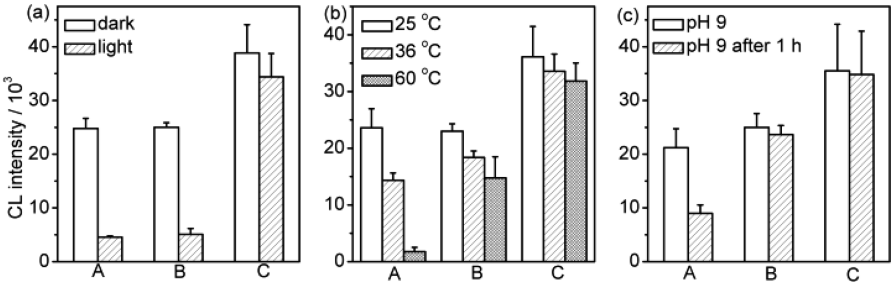

Figure 4. Effects of (a) light irradiation at room temperature for 1 h, (b) temperature in dark for 0.5 h, and (c) alkaline conditions in the dark for 1 h on CL intensity of the luminol-H_2O_2 reaction catalyzed by (A) HRP, (B) hemin/G-quadruplex DNAzyme, and (C) MnTMPyP-dsDNA.

dx.doi.org/10.1021/ac4000688 | Anal. Chem. 2013, 85, 3374−3379

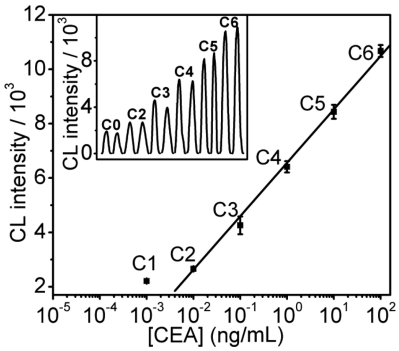

Figure 6. Calibration plot of the proposed method for CEA detection. Inset: dose−response curve. C0 to C6 corresponded to CEA concentrations of 0, 0.001, 0.01, 0.1, 1.0, 10, 100 ng/mL, respectively. Error bars were estimated from three parallel experiments.

comparable to other CL immunoassays using HRP[34] and DNAzyme as labels.[21] The sensitivity as the slope of the calibration plot was 1965.9 au, which was about 2 and 4 times larger than those of assay without HCR amplification (Figure S4, Supporting Information) and HRP/AuNP based CL immunoassay,[35] respectively.

Moreover the practical detection of human serum samples showed acceptable accuracy (Table 2). The high sensitivity, wide detection range, and good reliability indicated that the proposed MnTMPyP-dsDNA as a peroxidase-like mimic had great potential in practical application.

Table 2. Assay Results of Clinical Serum Samples Using the Proposed and Reference Methods

sample no.	1	1[a]	1[b]	2	3
proposed method (ng/mL)	6.71	0.699	0.063	2.15	3.96
reference method (ng/mL)	6.86	6.86	6.86	2.06	3.60
relative error (%)	−2.19	1.90	−8.16	4.37	10.0

[a]The serum samples were diluted at 10 times. [b]The serum samples were diluted at 100 times.

CONCLUSIONS

The MnTMPyP-dsDNA complex can be conveniently synthesized, functionalized, and combined with a HCR process for signal amplification. It possesses high peroxidase-like catalytic activity and good affinity to the enzymatic substrate. The catalytic activity is higher than that of hemin/G-quadruplex DNAzyme. MnTMPyP-dsDNA as mimicking enzyme of HRP shows much quicker catalytic kinetics and better stability in the conditions exposing to light irradiation and high temperature than both HRP and DNAzyme. It also possesses better stability than HRP at high pH. The groove binding of MnTMPyP to dsDNA scaffold can efficiently maintain the activity of the catalytic center, MnTMPyP, meanwhile improve the ability to resist the effect of H_2O_2 on the catalytic activity. By combining with an isothermal HCR process, the mimicking enzyme can grow on a support to achieve CL signal amplification and perform a highly sensitive CL detection. Because of the outstanding advantages of MnTMPyP-dsDNA, this novel enzyme mimic can be extended to combine with other amplification strategies and nanomaterial carriers for application in different fields.

ASSOCIATED CONTENT

Supporting Information

Additional information as noted in text. This material is available free of charge via the Internet at http://pubs.acs.org.

AUTHOR INFORMATION

Corresponding Author

*Phone/fax: +86-25-83593593. E-mail: wujie@nju.edu.cn (J.W.); hxju@nju.edu.cn (H.J.).

Notes

The authors declare no competing financial interest.

ACKNOWLEDGMENTS

We gratefully acknowledge the National Basic Research Program (Grant 2010CB732400), the National Natural Science Foundation of China (Grants 21105046, 21075055, 21135002, and 21121091), the PhD Fund for Young Teachers (Grant 20110091120012), the Natural Science Foundation of Jiangsu (GrantBK2011552), and the Leading Medical Talents Program from Department of Health of Jiangsu Province.

REFERENCES

(1) Dai, Z. H.; Liu, S. H.; Bao, J. C.; Ju, H. X. *Chem.—Eur. J.* **2009**, *15*, 4321−4326.
(2) Liu, X. Q.; Freeman, R.; Golub, E.; Willner, I. *ACS Nano* **2011**, *7*, 7648−7655.
(3) Guo, Y. J.; Deng, L.; Li, J.; Guo, S. J.; Wang, E. K.; Dong, S. J. *ACS Nano* **2011**, *5*, 1282−1290.
(4) Collman, J. P.; Boulatov, R. C.; Sunderland, J.; Fu, L. *Chem. Rev.* **2004**, *104*, 561−588.
(5) Xu, X.; Lu, H. J.; Ruppel, J. V.; Cui, X.; Mesa, S. L. D.; Wojtas, L.; Zhang, X. P. *J. Am. Chem. Soc.* **2011**, *133*, 15292−15295.
(6) Cong, Z. Q.; Kurahashi, T.; Fujii, H. *J. Am. Chem. Soc.* **2012**, *134*, 4469−4472.
(7) Zhang, G. F.; Dasgupta, P. K. *Anal. Chem.* **1992**, *64*, 517−522.
(8) Bruice, T. C. *Acc. Chem. Res.* **1991**, *24*, 243−249.
(9) Wang, Q. G.; Yang, Z. M.; Zhang, X. Q.; Xiao, X. D.; Chang, C. K.; Xu, B. *Angew. Chem., Int. Ed.* **2007**, *46*, 4285−4289.
(10) Wang, Q. G.; Yang, Z. M.; Ma, M. L.; Chang, C. K.; Xu, B. *Chem.—Eur. J.* **2008**, *14*, 5073−5078.
(11) Yamaguchi, H.; Tsubouchi, K.; Kawaguchi, K.; Horita, E.; Harada, A. *Chem.—Eur. J.* **2004**, *10*, 6179−6186.
(12) Fruk, L.; Niemeyer, C. M. *Angew. Chem., Int. Ed.* **2005**, *44*, 2603−2606.
(13) Chen, J.; Zhao, L.; Bai, H.; Shi, G. *J. Electroanal. Chem.* **2011**, *657*, 34−38.
(14) Xue, T.; Jiang, S.; Qu, Y. Q.; Su, Q.; Cheng, R.; Dubin, S. C.; Chiu, Y.; Kaner, R.; Huang, Y.; Duan, X. F. *Angew. Chem., Int. Ed.* **2012**, *51*, 3822−3825.
(15) Travascio, P.; Witting, P. K.; Mauk, A. G.; Sen, D. *J. Am. Chem. Soc.* **2001**, *123*, 1337−1348.
(16) Pelossof, G.; Tel-Vered, R.; Elbaz, J.; Willner, I. *Anal. Chem.* **2010**, *82*, 4396−4402.
(17) Yuan, Y. L.; Gou, X. X.; Yuan, R.; Chai, Y. Q.; Zhuo, Y.; Mao, L.; Gan, X. X. *Biosens. Bioelectron.* **2011**, *26*, 4236−4240.
(18) Yin, X. B. *TrAC, Trends Anal. Chem.* **2012**, *33*, 81−94.
(19) Deng, M. G.; Zhang, D.; Zhou, Y. Y.; Zhou, X. *J. Am. Chem. Soc.* **2008**, *130*, 13095−13102.
(20) Xiao, Y.; Pavlov, V.; Gill, R.; Bourenko, T.; Willner, I. *ChemBioChem* **2004**, *5*, 374−379.
(21) Wang, C.; Wu, J.; Zong, C.; Ju, H. X.; Yan, F. *Analyst* **2011**, *136*, 4295−4300.
(22) Groves, J. T. *J. Porphyrins Phthalocyanines* **2000**, *4*, 350−352.
(23) Motsenbocker, M.; Ichimori, Y.; Kondo, K. *Anal. Chem.* **1993**, *65*, 397−402.

(24) Pasternack, R. F.; Gibbs, E. J.; Villafranca, J. J. *Biochemistry* **1983**, *22*, 2406−2414.
(25) Kuroda, R.; Tanaka, H. *J. Chem. Soc. Chem. Commun.* **1994**, 1575−1576.
(26) Gandini, S. C. M.; Yushmanov, V. E.; Perussi, J. R.; Tabak, M.; Borissevitch, I. E. *J. Inorg. Biochem.* **1999**, *73*, 35−40.
(27) Nitta, Y.; Kuroda, R. *Biopolymers* **2006**, *81*, 376−391.
(28) Dirks, R. M.; Pierce, N. A. *Proc. Natl. Acad. Sci. U.S.A.* **2004**, *101*, 15275−15278.
(29) Liu, H.; Fu, Z. F.; Yang, Z. J.; Yan, F.; Ju, H. X. *Anal. Chem.* **2008**, *80*, 5654−5659.
(30) Schwalb, N. K.; Temps, F. *Science* **2008**, *322*, 243−245.
(31) Kumar, C. V.; Asuncion, E. H. *J. Am. Chem. Soc.* **1993**, *115*, 8547−8553.
(32) Araki, K.; Silva, C. A.; Toma, H. E.; Catalani, L. H.; Medeiros, M. H. G.; Mascio, P. D. *J. Inorg. Biochem.* **2000**, *78*, 269−273.
(33) Lei, J. P.; Ju, H. X.; Ikeda, O. *Electrochim. Acta* **2004**, *49*, 2453−2460.
(34) Chen, L. L.; Zhang, Z. J.; Zhang, X. M.; Fu, A. H.; Xue, P.; Yan, R. F. *Food Chem.* **2012**, *135*, 208−212.
(35) Zong, C.; Wu, J.; Wang, C.; Ju, H. X.; Yan, F. *Anal. Chem.* **2012**, *84*, 2410−2415.